LA-UR-97- 313

TITLE: **THE DYNAMIC RESPONSE OF INELASTIC DELAMINATED COMPOSITE PLATES**

AUTHOR(S): Todd O. Williams, T-3
Frank L. Addessio, T-3

SUBMITTED TO: *International Conference on Composite Materials, Gold Coast Australia, July 14–18, 1997*

Los Alamos

Los Alamos National Laboratory
Los Alamos, New Mexico 87545

FORM NO. 836 R4
ST. NO. 2629 5/81

CONF-970735--2
LA-UR--97-313

THE DYNAMIC RESPONSE OF INELASTIC, DELAMINATED COMPOSITE PLATES

Todd O. Williams,[1] **Frank L. Addessio**[1]

[1]*T-3 Theoretical Division*
Los Alamos National Laboratory
Los Alamos, New Mexico 87545, USA

SUMMARY. The dynamic behavior of metal matrix composite (MMC) plates is considered. In particular, the influence of inelastic deformations and delamination at the interfaces of the lamina on the macroscopic and local response of Al_2O_3/Al plates are studied. The work is carried out using a recently developed plate theory which models both delamination and localized history-dependent effects such, as inelasticity. A linear debonding model for the interface is employed for the current work. The theory models both the initiation and growth of delaminations without imposing any restrictions on the location, size, or direction of growth of the delamination. In the current work the response of the individual lamina in the plate are modelled using the Method of Cells (MOC) micromechanical model. The inelastic behavior in the matrix is modelled using the unified viscoplastic theory of Bodner and Partom.

The behavior of a Al_2O_3/Al plate under dynamic cylindrical bending subjected to a ramp and hold type of loading is examined. For simplicity, the plate is assumed to be composed of a cross-ply layup. It is shown that both inelastic deformations and delamination have a strong influence on dynamic plate behavior. The inelastic deformations have stronger effect on the axial displacement while delamination has greater influence on the deflection.

KEYWORDS: Delaminated composite plates, interfacial constitutive laws, dynamic plate behavior, micromechanics, Method of Cells, Viscoplasticity

INTRODUCTION

Laminated composite structures have many potential applications in a variety of engineering fields. However, laminated structures are susceptible to delaminations between layers. The presence of delaminations can cause significant degradation of the structural response characteristics, as compared to perfectly bonded structures. Additionally, it must be recognized that history-dependent inelastic deformations evolve in composite plates under many loading situations. Furthermore, these mechanisms can be highly interactive. Therefore, it is necessary that analytical tools which can accurately predict these effects must be developed and subsequently employed in the design and analysis process.

A review of work which considers the inelastic dynamic behavior of homogeneous plates is given in [1]. More recently, work has been done to study the inelastic behavior of composite plates [2]. To date, relatively little work has been done considering the dynamic behavior of inelastic delaminated composite plates.

One potential method for analyzing delamination initiation and growth is through the use of interfacial constitutive models [3-6] The general form of such constitutive relations are given by

$$\Delta_i = f_i(\Delta_i, t_i) \tag{1}$$

where Δ_i are the displacement jumps and t_i are the interfacial tractions. The relationship of these types of models to fracture mechanics is provided in [6].

A recently developed plate formulation is employed to study the dynamic behavior of inelastic delaminated composite plates [7,8]. The plate theory is based on an approximate higher-order discrete layer analysis. The theory is capable of incorporating any general nonlinear interfacial model behavior in an internally consistent fashion. No assumptions concerning the location, direction of growth, or number of delaminations are made in the theory. The plate theory is sufficiently general that any inelastic constitutive model can be employed. The plate theory has been shown to provide excellent agreement with both exact static elastic solutions and approximate dynamic solutions [7,8].

PLATE THEORY FORMULATION

Consider a single layer. It is assumed that the displacement field within this layer is approximated by

$$u_i(x,y,z,t) = V_i^j(x,y,t)\,\phi^j(z) \tag{2}$$

where $j = 1,2,\ldots,N$. N is the order of the polynomial expansion. The functions $\phi^j(z)$ are specified functions of the transverse coordinate z and the $V_i^j(x,y,t)$ are the associated displacement coefficients. The governing equations for the layer are obtained by substituting the above displacement field into the principle of virtual work

$$\tau_i^j + N_{i\alpha,\alpha}^j - R_i^j + F_i^j = I^{mj}\dot{v}_i^m \tag{3}$$

where $m, j = 1,2,\ldots,N$. The corresponding inplane boundary conditions are

$$V_i^j = \text{ specified on } \partial\Omega_1 \tag{4a}$$

$$T_i^j = N_{i\alpha}^j n_\alpha \quad \text{on } \partial\Omega_2 \tag{4b}$$

where $\partial\Omega = \partial\Omega_1 + \partial\Omega_2$ and $\partial\Omega$ is the plate boundary. Explicit satisfaction of both the continuity of the interfacial tractions and the jump conditions on the interfacial displacements are utilized to couple the equations governing the behavior of different layers to obtain the governing equations for the laminate. These interfacial conditions are given by

$$\left(V_i^l\right)^{k+1} - \left(V_i^N\right)^k = \Delta_i^k = f_i\left(\Delta_i{}^k, \tau_i{}^k\right) \tag{5a}$$

$$\left(\tau_i^j\right)^k + \left(\tau_i^j\right)^{k+1} = 0 \tag{5b}$$

The above results are completely general and the displacement jumps are expressed in a direct and consistent fashion as a function of the fundamental unknowns in the theory, V_i^j and τ_i^j. Additionally, the interfacial delamination relations can easily incorporate the constraint that the layers cannot interpenetrate.

The above formulation has been carried out in a sufficiently general fashion that any constitutive law for the behavior of the layer or interface may be incorporated and, therefore, any evolution laws for the local effects can be consistently incorporated into the formulation.

The general theory has been implemented in an explicit finite element (FE) code. In the FE code it is assumed that the temporal gradient in the equation of motion is approximated as

$$\dot{v} = \frac{v - v_0}{\Delta t} \tag{6}$$

where v_0 and Δt are the velocity at the preceding time and the time increment, respectively. Also the left hand side of the equation of motion is evaluated at the previous time step. It is noted that the gradient terms are evaluated using the Mean-Value Theorem.

$$\left\langle \frac{\partial \sigma_{iz}}{\partial x} \right\rangle_m \int \Psi^m d\Omega = \sum_n \left(\int \Psi^m \frac{\partial \Psi^n}{\partial x} d\Omega \right) \sigma_{iz}^n \tag{7}$$

Use of these expressions in the definitions of the force resultants, $N_{i\alpha}^j$ and R_i^j, then using these results in the governing equations as known forcing terms allows the new velocities for the layers to be determined. The new velocities are used to update the rate-of-deformation tensor using an expression based on the Mean-Value theorem similar to the above expression. The stresses throughout the plates are then updated by substituting the new rate-of-deformation tensor into the constitutive model for the materials within each layer. Once the stresses are computed, the boundary conditions for the plate are updated and the algorithm pursues advancing the velocities at the next time step. This process in continued until the problem is complete. Further details of the dynamic implementation of the theory are given in [8].

METHOD OF CELLS MODEL

The Method of Cells [3] represents an efficient and accurate micromechanical model for predicting the inelastic behavior of composite materials. The analysis considers the behavior of a composite composed of a doubly periodic array of fibers which implies that it is only necessary to model the behavior of a unit cell, Fig. 1. The unit cell is subsequently considered to consist of four subcells. A linear velocity expansion is used to model the behavior in each subcell.

$$\dot{u}_i^{(\alpha,\beta)} = \dot{w}_i^{(\alpha,\beta)} + \overline{x}_2 \phi_i^{(\alpha,\beta)} + \overline{x}_3 \psi_i^{(\alpha,\beta)} \tag{8}$$

where α and β are used to denote the subcells and $\overline{x}_2$ and $\overline{x}_3$ denote local sucell coordinates. Using the strain displacement relations the infinitesimal strains within each subcell can be expressed as functions of the $\phi_i^{(\alpha,\beta)}$ and the $\psi_i^{(\alpha,\beta)}$. Imposing the velocity and traction continuity conditions between subcells

$$h_1 l_\beta \dot{\epsilon}_{i2}^{(1,\beta)} + h_2 l_\beta \dot{\epsilon}_{i2}^{(2,\beta)} = h \dot{\epsilon}_{i2}^o \quad \text{for i=1,3}$$
$$h_\alpha l_1 \dot{\epsilon}_{i3}^{(\alpha,1)} + h_\alpha l_2 \dot{\epsilon}_{i3}^{(\alpha,2)} = l \dot{\epsilon}_{i3}^o \quad \text{for i=1,3}$$
$$\sum_{\alpha,\beta=1}^{2} v_{(\alpha,\beta)} \dot{\epsilon}_{23}^{(\alpha,\beta)} = V \dot{\epsilon}_{23}^o \tag{9}$$
$$\sigma_{i2}^{(1,\beta)} = \sigma_{i2}^{(2,\beta)}$$
$$\sigma_{i3}^{(\alpha,1)} = \sigma_{i3}^{(\alpha,2)}$$

in conjunction with the periodicity of the velocity fields provides closed form expressions for the effective macroscopic constitutive relations for a composite.

$$\dot{\overline{\sigma}} = \mathbf{C}^{eff} \dot{\epsilon}^o - \mathbf{\Gamma}^{eff} \tag{10}$$

BODNER-PARTOM VISCOPLASTIC MODEL

The simplest form of the unified viscoplastic theory of Bodner and Partom [9] is used to model the inelastic behavior of the matrix phase in the composite. The fiber is assumed to be elastic. A Prandtl-Reuss type flow rule is used in this theory.

$$\dot{\epsilon}_{ij}^I = \Lambda s_{ij} \tag{11}$$

where

$$\Lambda = \left(\frac{D_2^I}{J_2}\right)$$
$$D_2^I = D_o^2 exp\left[-\left(\frac{A^2}{J_2}\right)^n\right] \tag{12}$$
$$A^2 = \frac{1}{3} Z^2 \left(\frac{n+1}{n}\right)^{\frac{1}{n}}$$
$$Z = Z_1 - (Z_1 - Z_o)\, exp\,(-mW_p/Z_o)$$

where $\dot{\epsilon}_{ij}^I$ is the inelastic strain rate, W_p is the plastic work, and $J_2 = \frac{1}{2} s_{ij} s_{ij}$ and $s_{ij} = \sigma_{ij} - \frac{1}{3}\sigma_{kk}\delta_{ij}$. The material viscoplastic response is characterized by the constants n, m, D_o, Z_o, and Z_1. The Bodner-Partom theory as presented models the inelastic material behavior using isotropic hardening only.

RESULTS

For this work the dynamic response of a cross-ply (0/90) composite plate subjected to cylindrical bending is examined. The aspect ratio of the plate is 5. Thus the plate can be consider to be a thick plate. In such a plate significant transverse stresses are observed. The plate is composed of alumina fibers Al_2O_3 embedded in an alumimun matrix. The fiber is elastic and the matrix supports inelastic deformation. The material properties of the constituent phases are given in Table 1. A fiber volume fraction of 64% is used generate the results. The plate is subjected to a ramping half sine load for 1 μs where the peak value changes from 0 to $q_0 = 1$ GPa. The load is subsequently held at this peak value for 4 μs.

TABLE 1. Material properties for Al_2O_3/Al constituents.

Material	E (GPa)	ν	ρ (g/cm^3)	$D_o(1/s)$	Z_0 (MPa)	Z_1 (MPa)	m	n
Al_2O_3	398.7	0.236	3.97	–	–	–	–	–
Al	72.0	0.345	2.70	10^5	340	435	300	10

Three cases are considered. In the first case the plate is modelled as inelastic but perfectly bonded (PB). In case 2 both inelastic behavior and debonding (DB) are modelled. For this case, a linear interfacial constitutive model is employed for simplicity, ($\Delta_i = R\tau_i$), where the τ_i are the appropriate interfacial stresses obtained directly from the theory. The interfacial model parameters for the debonded analysis are $R_n = R_s = 0.1$ cm/GPa where the subscipts n and s denote the normal and shearing responses. Initially the laminate in case 2 is perfectly bonded. The final case models the plate as elastic and perfectly bonded.

The transverse displacement as a function of time for the three cases is given in Fig. 1. The following discussion is based on simple 1D wave propagation arguments considering the effects of the internal waves. The quoted times apply to case 3 (the elastic, perfectly bonded case). The transverse sound speed in the lamina is about 0.8. The transverse sound speed of the lamina is about 0.8 cm/μs. Initially, the top surface of the plate is rapidly accelerated by the applied loading. Both the interface and the bottom surface remain at rest. At approximately 1.2 μs the maximum amplitude of the wave reaches the interface. The presence of the interface results in a reflected wave in the top lamina and a transmitted wave in the bottom lamina. The initial transmitted waves due to the beginning of the applied loading reach the outer surfaces of the plate at this time. This begins a rapid acceleration of the back surface. The reflected waves at the top surface begin to cause some deceleration of this surface. At approximately 2 μs the initial wave reflections from the outer surfaces reach the interface. The midsurface of the plate then begins to accelerate. Additionally, at this point in time, the maximum wave amplitude has reached the outer surfaces of the plate. This results in the greatest acceleration at the bottom surface and rapid deceleration of the top surface. Similar wave reflection and interaction process continues throughout the rest of the calculations and corresponding interpretations of the wave effects can be made.

Incorporating inelastic deformations into the calculation, case 1, results in similar effects in the deflection versus time response. However, the trends occur at delayed times as compared to case 3. The delays in the trends are due to the fact that the inelastic deformations migitate the effects of the elastic waves. The presence of the inelastic deformations "soften" the plate and result in larger deformation magnitudes. The amount of delay in case 1 as compared to case 3 is relatively small due to the relatively large volume fraction of the elastic fiber. If the fiber were inelastic or a lower fiber volume fraction were considered then the delays in the effects due to the presence of inelastic deformations would be larger.

Consideration of the response for case 2 (debonding and inelastic deformations) shows that the presence of delamination results in the same trends as cases 1 and 2. Similar to case 1, the trends are delayed as compared to case 1. These delays are greater than those observed in case 1. The presence of the debonding at the interface results in an impedance mismatch. This impedance results in stronger reflected wave effects within the top lamina and weaker transmitted wave effects in the bottom lamina. As the value of R increases the impedance becomes larger and the reflected wave effects become stronger. Large values of R result in the plate approaching the debonded state with the top lamina being ejected as a solid body. In general, the displacement magnitudes are larger for case 2 than for cases 1 and 3. This is consistent with the "softer" behavior induced by the presence of both the inelastic deformations and the debonding. It is evident from these results that the presence of delamination results in displacement jumps across the interface which are significant in comparison with the variation of the displacement change across the laminate at various times. Examination of all three sets of results indicates that for the current laminate debonding has a larger effect on the response than plasticity.

The distributions of the axial displacement through the thickness at the end of the plate for all three cases are given in Fig. 2. It is evident from these results that both plasticity and debonding have a strong impact on the plate deformation at the local level. The largest deviations due to the presence of these effects occur in the region around the midplane of the plate. The maximum deviation between cases 2 and 3 does occur at the midplane and represents about 61% of the total variation in the distribution. The presence of plasticity has a relatively stronger influence on the axial displacement than does the presence of delamination. Consideration both plasticity and delamination only results in an additional variation, as compared to case 1, of about 13%. The displacement jump in case 2 due to delamination represents about 10% of the overall variation in the distribution.

The transverse displacement distributions through the thickness of the plate at the middle of the plate for all three cases are given in Fig. 3. The presence of plasticity has a much smaller effect on the deflection than was seen in the axial displacements. The maximum deviation from distribution of case 3 is 5%. The presence of the delamination has a more significant impact on the deflection than observed for the axial displacement. In this case, the maximum deviation from the case 3 distributions is about 30%. The jump due to delamination represents about 22% of the variation in the deflection distribution.

Finally, the transverse stress distributions through the thickness of the plate for all three cases at the middle of the plate are given in Fig. 3. As was observed in the deflection distributions, the presence of plasticity has a much smaller influence on the transverse stress as compared to the presence of the delamination. The maximum deviations between the distributions for cases 1and 3 is about 0.07 while a maximum deviation of about 0.57 is observed between cases 2 and 3.

CONCLUSIONS

A discrete layer plate theory has been used to consider the relative influence of both inelastic deformations and delamination on the dynamic behavior of a 0/90 Al_2O_3/Al plate. The inelastic deformations of the composite were modelled using the Bodner-Partom viscoplastic theory in the micromechanical models known as the Method of Cells. A simple linear debonding model for the interfacial behavior was used in this study.

It was seen that the presence of plasticity and delamination have a significant effect on both the macroscopic and local behavior of the plate. Consideration of the macroscopic behavior indicated that the delamination had a stronger influence than the inelastic deformations. This was in part due to the fact that the debonding at the interface acted as an impedance which results in stronger wave effects in the top lamina as compared to the bottom lamina. Consideration the effects of delamination and plasticity on the local behavior indicated that these phemenona had different influences. The presence of inelasticity had a stronger influence on the axial displacement than did the presence of delamination. Alternatively, the presence of the delamination had a much stronger influence on the deflection and the transverse stress than did inelasticity.

REFERENCES

1. Jones, N. "Recent Studies on the Dynamic Plastic Behavior of of Structures", *Appl. Mech. Rev.*, Vol. 42, pp 95

2. Gilat and Aboudi, "Dynamic Buckling of Metal Matrix Composite Plates and Shells under Cylindrical Bending", *Comp. Struct.*, Vol. 28, 1994, pp 459

3. Aboudi, J. "The Mechanics of Composite Materials: A Unified Micromechanics Approach", Elsevier Science Publishers B.V., Amsterdam, The Netherlands, 1991

4. Needleman, A. "A Continuum Model for Void Nucleation by Inclusion Debonding", *J. Appl. Mech.*, Vol. 54, 1987, pp 525

5. Needleman, A. "An Analysis of Decohesion along an Imperfect Interface", *Int. J. Fract.*, Vol. 42, 1990, pp 21

6. Corigliano, A. "Formulation, Identification, and Use of Interface Models in the Numerical Analysis of Composite Delaminations", *IJSS*, Vol. 30, 1993, pp 2779

7. Williams, T.O. and Addessio, F.L. "A General Theory for Laminated Plates with Delaminations", *IJSS*, (in press), 1997 (also available as a LANL internal report, LA-UR-96-2593)

8. Williams, T.O. and Addessio, F.L. "Dynamic Behavior of Laminated Plates with Delaminations", *IJSS*, (in submission), 1997 (also available as a LANL internal report, LA-UR-96-3110)

9. Bodner, S.R. and Partom, Y. "Constitutive Equations for Elastic-Viscoplastic Strain Hardening Materials", *J. Appl. Mech.*, pp 385

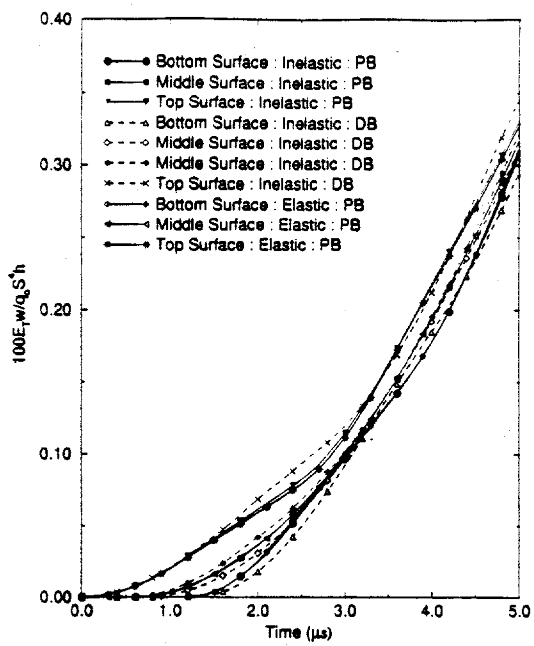

Figure 1 Transverse displacement at the middle of the plate as a function of time.

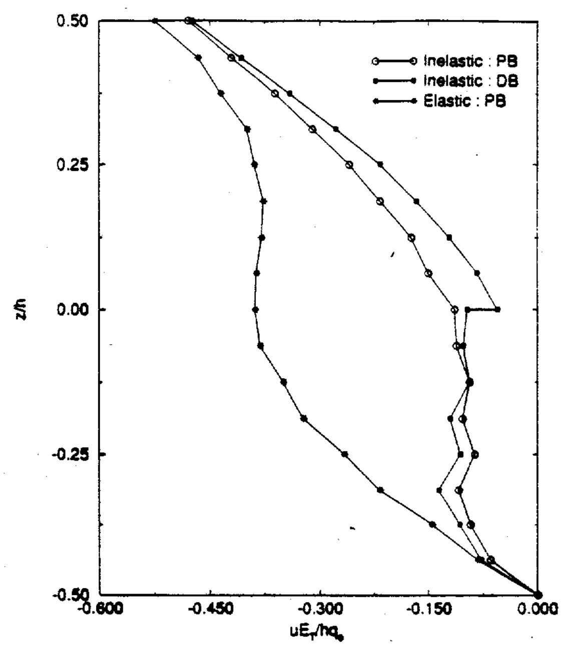

Figure 2. Through the thickness distributions of the axial displacement at the end of the plate.

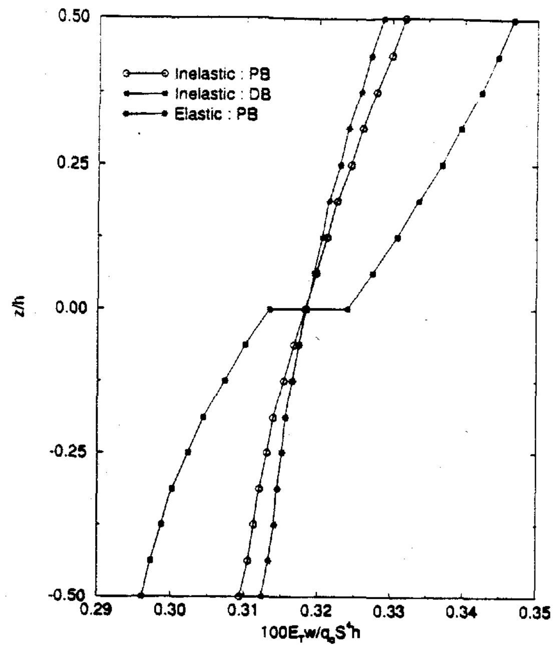

Figure 3. Through the thickness distributions of the deflection at the middle of the plate.

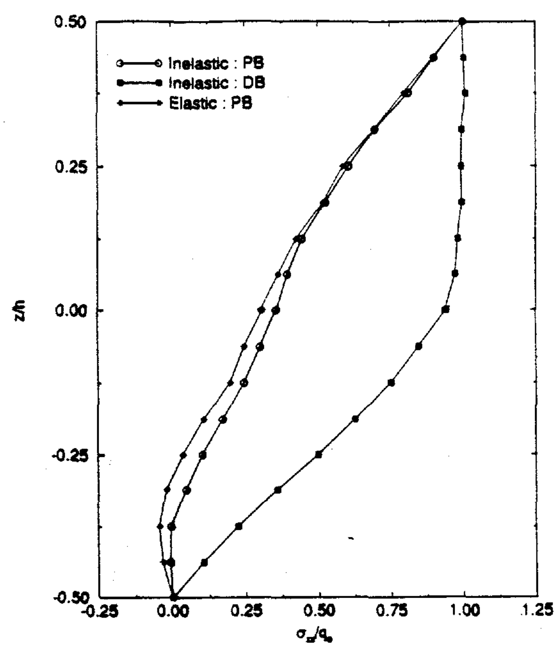

Figure 4. Through the thickness distributions of the transverse stress at the middle of the plate.